American Mineralogist, Volume 69, pages 30–40, 1984

Mid- to late-stage kimberlitic melt evolution: phlogopites and oxides from the Fayette County kimberlite, Pennsylvania

ROBERT H. HUNTER,[1] RANDAL D. KISSLING, AND LAWRENCE A. TAYLOR

Department of Geological Sciences
University of Tennessee, Knoxville, Tennessee 37996

Abstract

Hypabyssal-facies kimberlite from Fayette County, Pennsylvania, comprises megacrysts/inclusions, peridotite xenoliths, and crustal fragments set in a matrix of phlogopite, spinel, ilmenite, perovskite, rutile, carbonate and minor serpentine. Two chemically distinct populations of megacrysts/inclusions are present: a Cr-rich suite (olivine(Fo 90–93), Cr-pyrope, Cr-diopside, enstatite, Cr-spinel, and immiscible sulfide melt products); and a Cr-poor suite (olivine (Fo 81–85), pyrope, diopside, and picroilmenite (16–37 mol% $MgTiO_3$)). These minerals record the evolution of two chemically distinct kimberlitic melts within the low velocity zone (LVZ). Olivines of both populations have rims of Fo 88–89, and ilmenite megacrysts possess reverse-zoned rims (34–51 mol% $MgTiO_3$). These zonations reflect mixing of the two populations of megacrysts and their host melts within the LVZ.

The chemical evolution of this hybrid melt during mid- to late-stages of the kimberlite's history is recorded by groundmass phlogopites and oxides. Phlogopites document increases in activities of Fe*, Ca, and Na and a decrease in Cr-activity. Groundmass ilmenites are compositionally similar to ilmenite megacryst rims. Spinels show zonation from titanian Mg-Al-chromite (TMAC) through chromian Mg-Al-titanomagnetite (CMAT) to magnesian Al-titanomagnetite (MAT), reflecting increase in Ti and Fe^{3+} activities and decrease in activities of Cr and Mg during the evolution of the hybrid melt. Late-stage rutile indicates high activities of Ti and near-solidus temperatures. Ilmenite instability is a function of a late-stage increase in Ca activity with stabilization of Nb-, REE-bearing perovskite. Spinels reaction rims of ilmenite megacrysts are compositionally similar to CMAT in the groundmass; adjacent to the matrix, they are zoned to MAT. Inhomogeneous distribution of sulphides and perovskite in the groundmass and variable modal proportions of spinel and perovskite in the ilmenite megacryst reaction rims indicate local variations in fugacites of O_2, S_2, and CO_2.

Introduction

Typically, kimberlite consists of megacrysts, and their inclusions, and xenoliths all set in a matrix of oxides, phlogopite, serpentine, and carbonate (*e.g.*, Skinner and Clement, 1979; Dawson, 1980). The megacrysts and xenoliths record processes within the low velocity zone (LVZ) related to the genesis of kimberlite and its early stages of evolution. In this regard, the origin of the megacrysts and their inclusions has been the subject of considerable debate (*e.g.*, Nixon and Boyd, 1973; Eggler *et al.*, 1979; Gurney *et al.*, 1979, Pasteris *et al.*, 1979). There is less uncertainty about the origin of the groundmass phases; clearly, they are products of crystallization in the mid- to late-stages of kimberlite evolution. Since the evolution of a melt is usually a continuous process, there will be overlap of these various stages. However, it is often convenient to consider them separately for purposes of description and interpretation.

Oxide minerals (*i.e.*, ilmenite, spinels, perovskite and rutile) are abundant in the groundmass of kimberlitic rocks. Because these phases are intrinsically sensitive to changes in magma chemistry, temperature, and oxygen fugacity, they record details of the mid- to late-stages of evolution of kimberlitic melts. Other groundmass phases, especially phlogopite, are also sensitive to changes in magma chemistry. Therefore, a combined study of groundmass and oxide and phlogopite phases should permit a detailed reconstruction of the later-stages in the evolution of a kimberlitic melt. This approach has been used for other occurrences (*e.g.*, Elthon and Ridley,

[1] Present address: Grant Institute of Geology, University of Edinburgh, West Mains Road, Edinburgh, U.K.

0003–004X/84/0102–0030$02.00

1979; Mitchell, 1979) and is the rationale used in the present study of the Fayette County kimberlite, Pennsylvania. A companion paper (Hunter and Taylor, 1984) addresses the early stage of this kimberlite's development as interpreted from the megacrysts, inclusions, and peridotite nodules. Therein, two distinct suites of megacrysts/inclusions have been recognized, a Cr-rich suite (olivine, Cr-garnet, Cr-diopside, enstatite, Cr-spinel, and immiscible sulphide-melt phases), and a Cr-poor suite (olivine, ilmenite, Cr-poor garnet, and diopside). The chemistry of these megacrysts and inclusions has been interpreted in the context of a magma-mixing model. Integration of the results of both studies has provided a coherent scenario of the entire genesis and evolution of this kimberlite.

Geologic setting and general characteristics

The Fayette County kimberlite (Fig. 1) occurs as a narrow (1–2 m wide) dike, extending NW–SE for over 4 km, emplaced into coal-bearing sediments of Pennsylvanian age. It has been intruded into a pre-existing fault-zone that is transcurrent to the regional NE–SW striking structure (Roen, 1968). A K–Ar date of 185±10 m.y. has been reported for this kimberlite (Pimental *et al.*, 1975). Early studies of the intrusion were reported by Smith (1912), Sosman (1938), and Hickock and Moyer (1940).

The bulk of the exposed dike is relatively unweathered. However, in some parts, primary textures have been obscured by extensive alteration—olivine is pseudomorphed by serpentine and phlogopites are chloritized. The dike is composite with well-preserved internal contacts. Two facies occur in roughly equal proportions and form the bulk of the exposed dike. One is composed of abundant porphyritic olivine (≥2 mm), phlogopite, and spinels set in a matrix of carbonate, fine-grained phlogopite, and minor serpentine. The second major facies is strongly porphyritic with abundant megacrysts, up to 3 cm in size (olivine > garnet > ilmenite > phlogopite; inclusions comprise olivine, garnet, pyroxene, ilmenite, Cr-spinel, and sulfides) and rare peridotite xenoliths. Modally, oxides, phlogopite phenocrysts, and smaller olivines are less abundant in this facies than in the former; consequently, there is a greater abundance of matrix carbonate and phlogopite. In this facies, the majority of the megacrysts and xenoliths (both mantle- and crustal-derived) form the cores of autoliths, with rims up to 5 mm in width, in which groundmass phlogopite flakes are tangentially oriented to the nucleus. Texturally, the autoliths are similar to those described by Clement (1973), Ferguson *et al.* (1973), and Danchin *et al.* (1975) from kimberlites in Lesotho and South Africa. Along the contact between these two major facies, a non-porphyritic facies is present as a zone up to 1 cm in width. This contact zone is gradational into the matrix of the megacryst facies but has a sharp contact with the other facies; it is composed of flow aligned groundmass phlogopite laths oriented subparallel to the contact. Texturally, this contact facies shows a strong resemblance to the autoliths; indeed within the megacryst facies, when a megacryst occurs adjacent to the margin, its surrounding autolith may be continuous with the contact facies.

Thin veins, up to 5 mm wide cut through matrix, megacrysts, and xenoliths. They are composed of skeletal to euhedral carbonate crystals, with growth-directions normal to the vein walls, set in a matrix of optically uniform serpentine.

The lack of extensive brecciation and the dike-like form indicate that this kimberlite was emplaced passively, possibly with no explosive diatreme phase having ever occurred at least at its present level of exposure. The presence of distinct facies with internal contacts indicates that the dike was injected as successive pulses of magma. Thermal metamorphism of the wallrock and xenolithic coal and shale indicates that the kimberlite was emplaced at temperatures estimated to be between 500° and 600°C (Sosman, 1938).

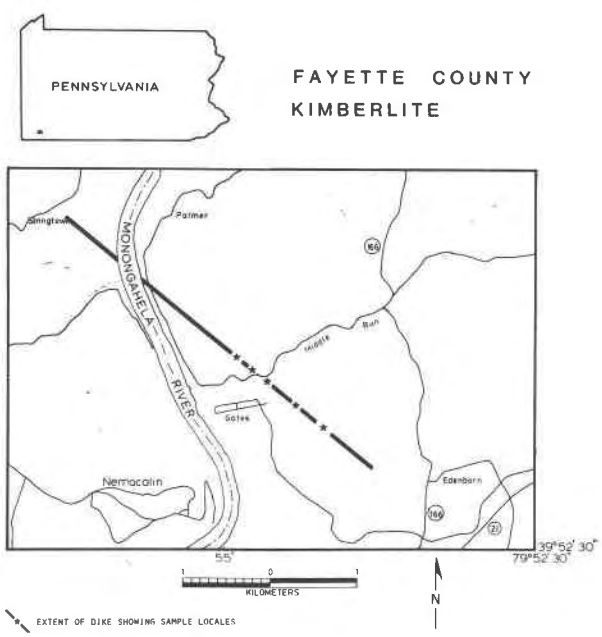

Fig. 1. Location of the Fayette County kimberlite.

Petrography and mineral chemistry of phlogopites and oxides

Mineral analyses were performed using an automated MAC 400S electron microprobe, utilizing the data reduction procedures of Bence and Albee (1968) and the data of Albee and Ray (1970). When grain-size permitted, 4–8 analyses were performed per grain. Representative analyses of phlogopites are presented in Table 1; no attempt to

Table 1. Representative phlogopite analyses

	Phenocryst core	Phenocryst rim	Garnet mantle core	Garnet mantle rim	Groundmass		Secondary mica in lherzolite
SiO_2	38.6 (6)*	36.9	36.2 (4)	35.5	37.5	35.6	37.8 (4)
TiO_2	4.52(5)	4.07	4.41(5)	3.94	3.51	2.59	3.51(9)
Al_2O_3	14.4 (1)	15.4	14.4 (3)	15.9	14.2	13.8	15.3 (3)
Cr_2O_3	1.52(4)	0.23	3.23(4)	0.41	0.17	0.03	1.46(4)
MgO	20.7 (2)	21.9	20.5 (2)	21.7	21.6	23.0	21.4 (2)
FeO**	4.89(12)	5.13	4.63(9)	5.51	5.77	7.22	4.45(18)
MnO	0.08(1)	0.08	0.04(1)	0.04	0.02	n.d.	0.08(3)
CaO	n.d.	0.11	0.02(1)	0.08	0.16	0.14	n.d.
Na_2O	0.33(2)	0.49	0.16(2)	0.32	0.39	0.42	0.55(5)
K_2O	9.85(7)	9.39	9.59	9.45	9.48	8.96	9.85(14)
Total	94.89	93.70	93.21	92.85	94.40	91.76	94.40

* Units in parentheses represent 1σ standard deviations of replicate analyses in terms of the last digit cited for the value to their immediate left, thus 38.6 (6) indicates a standard deviation of 0.6.
** All Fe is calculated as Fe^{2+}. n.d. = not detected (< 0.02%).

calculate Fe^{2+}/Fe^{3+} ratios was made. Representative oxide analyses are presented in Table 2; Fe_2O_3 in these phases has been calculated assuming stoichiometry.

Phlogopites

Phlogopite constitutes 20–30 modal % of the grains in the <1 mm size-range within this kimberlite. Four habits have been recorded: (1) euhedral to subhedral phenocrysts, 0.5–1.0 mm in size; (2) laths, typically 100 × 10 μm, within the groundmass; (3) mantles of subhedral, interlocking flakes surrounding garnet reaction assemblages; and (4) thin rinds of secondary phlogopite mantling garnet reactions within the lherzolite xenoliths. The phenocrysts possess normal pleochroism, and all have a distinct rim, 100–200 μm in width; the core region displays stronger absorption than the rims. The groundmass micas are optically similar to the phenocryst rims. Typically, the mantles on the garnet reaction rims are 200–500

Table 2. Representative ilmenite and spinel analyses

	Ilmenite megacryst core	Ilmenite megacryst rim	Grdmass ilmenite	CMAT inclusion	Grdmass CMAT	Grdmass CMAT	Grdmass MAT	CMAT megacryst reaction	CMAT megacryst lamallae	Cr-pleonaste garnet reaction
TiO_2	44.1 (5)	48.7 (5)	49.7 (5)	6.60(6)	13.7	19.8 (8)	9.58	21.4	20.3	0.40
Al_2O_3	0.18(2)	0.65(9)	0.63(2)	10.1 (1)	5.78	5.18(15)	6.57	5.90	2.07	57.8
Cr_2O_3	1.25(4)	2.65(16)	3.70(30)	37.4(2)	15.2	1.20(20)	0.03	1.59	4.10	8.67
Fe_2O_3	19.8	14.3	12.2	14.3	27.3	30.5	47.4	26.5	27.9	3.57
MgO	7.29(7)	14.3 (2)	13.9 (1)	13.7 (4)	13.2	12.8 (3)	9.94	13.1	10.1	20.5
FeO	20.6 (3)	17.9 (3)	19.8 (2)	17.1 (3)	24.2	30.2 (8)	25.0	31.9	34.5	8.39
MnO	0.29(2)	0.49(2)	0.43(1)	0.36(2)	0.70	0.62(5)	0.84	0.64	0.35	0.26
Total	99.51	98.99	100.36	98.96	100.08	100.30	99.31	101.03	99.32	99.59
Cation basis	(3)	(3)	(3)	(4)	(4)	(4)	(4)	(4)	(4)	(4)
Ti	0.802	0.841	0.853	0.147	0.343	0.497	0.248	0.532	0.545	0.007
Al	0.005	0.018	0.017	0.388	00.227	0.204	0.267	0.229	0.052	1.765
Cr	0.024	0.048	0.066	0.968	0.399	0.032	0.001	0.042	0.082	0.182
Fe3+	0.361	0.248	0.208	0.351	0.684	0.767	1.229	0.657	0.771	0.070
Mg	0.263	0.490	0.472	0.668	0.653	0.639	0.511	0.642	0.463	0.789
Fe2+	0.539	0.345	0.376	0.468	0.674	0.843	0.719	0.880	1.076	0.181
Mn	0.006	0.010	0.008	0.010	0.020	0.018	0.025	0.018	0.011	0.006
Σ	2.000	2.000	2.000	3.000	3.000	3.000	3.000	3.000	3.000	3.000

*Units in parentheses represent 1σ standard deviations of replicate analyses in terms of the last digit cited for the value to their immediate left, thus 44.1 (5) indicates a standard deviation of 0.5.
** Fe3+ is calculated assuming stoichiometry.

μm wide. These mantles are *not* kelyphitic rims; they are texturally different from the reaction assemblages described below. Within these mantles, the phlogopite flakes interlock; where crystals protrude into the matrix, they possess euhedral to subhedral outlines with an optically distinct rim as in the phenocrysts. Both these mantles on garnet megacrysts and the phenocrysts contain euhedral inclusions of Cr-spinel.

The TiO_2, FeO* (total Fe as FeO), and Cr_2O_3 contents of the phlogopites are plotted in Figure 2. Chemically, the cores of individual phenocrysts are homogeneous, with 1.3–1.8% Cr_2O_3, 4.5–5.0% TiO_2, and 4.6–5.5% FeO*. The rims contain 0.1–1.0% Cr_2O_3, 3.6–4.5% TiO_2, and 4.9–6.0% FeO*. The groundmass micas have low Cr_2O_3 contents (<0.2%) which overlap the compositions of the phenocryst rims, however, they exhibit a wider range in TiO_2 (1.7–4.5%) and FeO* (5.4–8.3%). In general, the phlogopite compositional range within the garnet megacryst mantles overlaps that of the phenocryst cores and rims, but the cores possess up to 3.2% Cr_2O_3. The secondary phlogopites in the lherzolites contain similar Cr_2O_3 contents to the cores of the phenocrysts but have markedly less TiO_2 (3.7%) and slightly less FeO* (4.0–4.5%). Within the phlogopites as a whole, there appears to be no systematic variability of Al_2O_3, MgO, or K_2O. However, there is a systematic change in minor components associated with the different parageneses. Phenocryst cores generally contain CaO concentrations near nominal detection limits for routine analysis (0.02%) and Na_2O in the range 0.20–0.30%. The rims and groundmass laths contain 0.09–0.18% CaO and 0.28–0.55% Na_2O; within the lherzolites, the secondary phlogopites range in Na_2O from 0.55 to 0.60%.

Micas in kimberlites show wide variations in chemical composition (*e.g.*, Smith *et al.*, 1978; Delaney *et al.*, 1980). Comprehensive studies of kimberlitic micas (*i.e.*, micas *not* related to mantle-derived xenoliths) have been reported from South African kimberlites (Smith *et al.*, 1978; 1979; Boettcher *et al.*, 1979; Elthon and Ridley, 1979; Boctor and Boyd, 1982) and from Canadian kimberlites (Smith *et al.*, 1978; Mitchell, 1979). Kimberlitic phlogopite analyses have also been reported by Rimsaite (1971), Clarke and Mitchell (1975), Emeleus and Andrews (1975), and Garrison and Taylor (1980). Compositions comparable to the phenocryst and groundmass phlogopites in the Fayette County kimberlite can be found in all the above cited papers. However, the systematic variability observed in the present study has not been described previously. Smith *et al.* (1978) found no correlation of Cr_2O_3, TiO_2 and FeO* among their Type II micas in individual South African kimberlites. Typically, kimberlitic phlogopite compositions show considerable scatter on inter-element plots. The correlation of chemistry with inferred crystallization sequence in the Fayette County kimberlite suggests that the mica compositions were changing in response to chemical changes in the fractionating melt. There is a decrease in TiO_2 from cores to rims of phenocryst phlogopites and a TiO_2 depletion recorded in the groundmass phlogopites. The paragenetic sequence observed in the oxide phases (see below) indicates an increase in aTi with fractionation, culminating in crystallization of rutile above the solidus. The decrease in TiO_2 in the phlogopites implies that phlogopite was not controlling TiO_2 in the fractionating melt, but was simply an indicator phase for changes in TiO_2. The depletion of Cr_2O_3 in the phlogopites is probably a consequence of

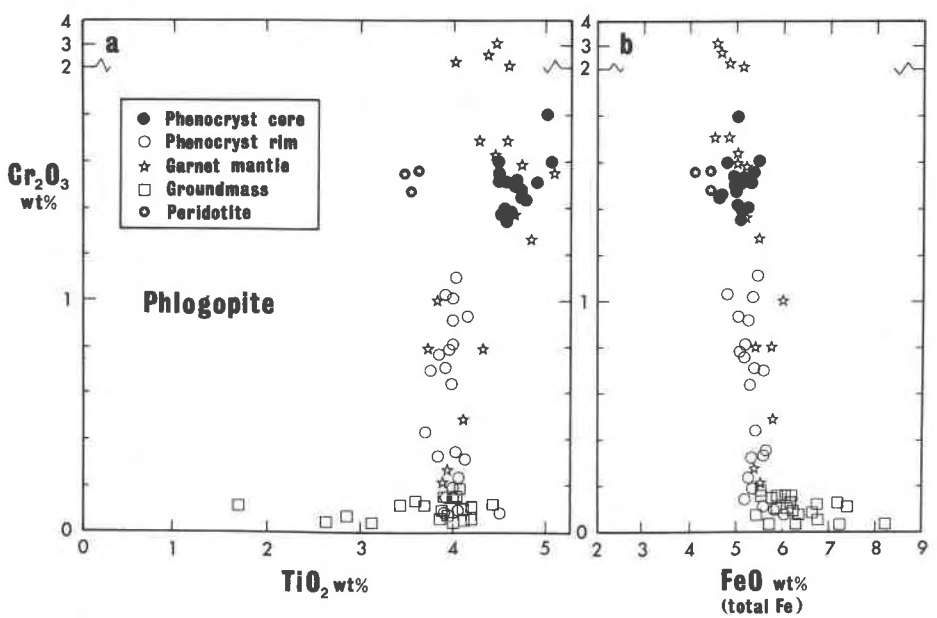

Fig. 2. Plots of Cr_2O_3 *vs.* TiO_2 and Cr_2O_3 *vs.* FeO* for phlogopites.

depletion in the fractionating melt by the Cr-bearing spinels. In addition, the phlogopites record an increase in the activities of Fe, Ca, and Na during fractionation.

Ilmenite

In the Fayette County kimberlite, ilmenite is present in several habits: rounded megacrysts, up to 1.5 cm in size; euhedral inclusions, 20–50 μm in size, in Cr-poor garnets; rounded inclusions in the rims of olivines; and as subhedral to rounded grains in the groundmass. The garnet inclusions are compositionally similar to the megacryst cores. Their chemistry has been described in detail in the companion paper; in summary, they contain 16–37 mol% $MgTiO_3$ and 0.05–2.05% Cr_2O_3. The megacrysts possess reverse-zoned rims (34–51 mol% $MgTiO_3$; 1.4–3.6% Cr_2O_3). The core-rim compositional profile is smooth with the zonation confined to the outer 200–300 μm.

All the ilmenite megacrysts possess reaction rims composed of spinel and perovskite (Fig. 3a,b, and d). The width of the reaction rim ranges from 20–200 μm from megacryst to megacryst but is of uniform width within a particular grain. Contacts with spinel and perovskite (see below) are irregular. Commonly, isolated patches of ilmenite are preserved in the spinel (Figs. 3a and d). The majority of these unreacted ilmenites are in optical continuity with the host ilmenite. However, where they are not, the ilmenite and mantling spinel are isolated from the rim (Fig. 3a); these cases reflect either dissaggregation of the reaction rim with subsequent epitaxial growth of spinel or groundmass ilmenites precipitating coincidentally close to the reaction rim. Occasionally, sulfides are concentrated in the matrix in close proximity to the ilmenite reaction rims (Fig. 3b).

Characteristically, ilmenite in the groundmass occurs as subhedral to rounded grains in the cores of spinels. In a few instances, a subhedral core region of grey-blue spinel

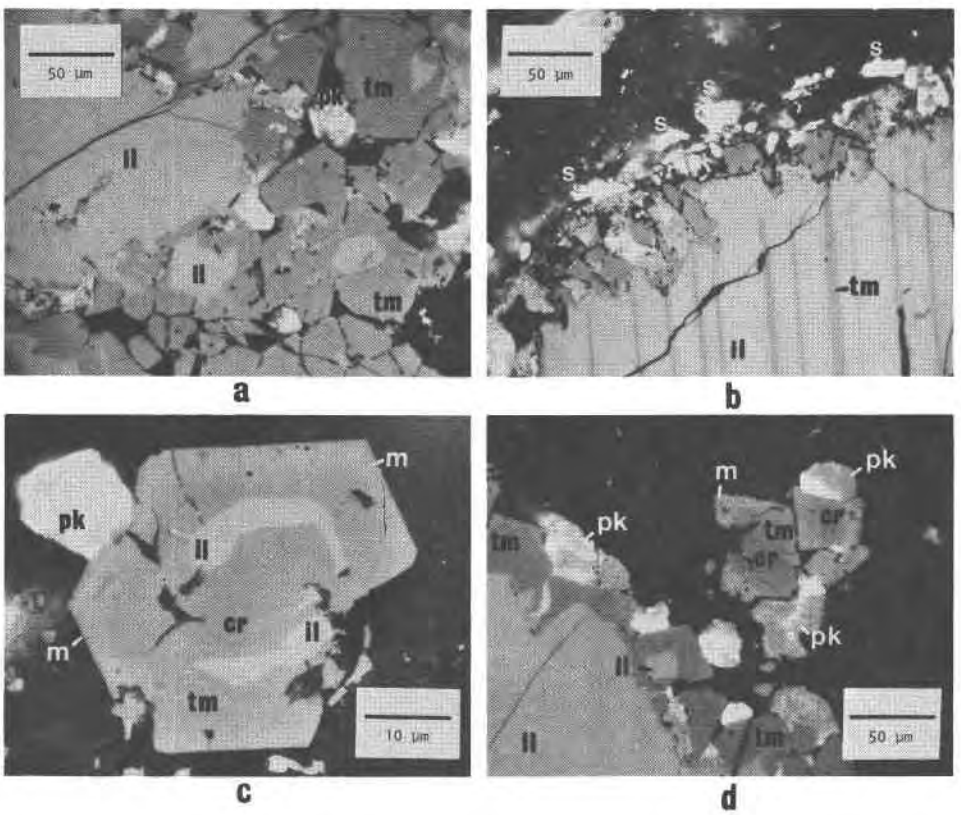

Fig. 3. Photomicrographs of oxide textures (all with plane-polarized, reflected light under oil-immersion; il = ilmenite; cr = TMAC; tm = CMAT; m = MAT; pk = Perovskite; s = sulfides). (a) ilmenite megacrysts reaction rim with perovskite and CMAT. An unreacted remnant of ilmenite is surrounded by spinel, some of which possesses euhedral, epitaxial overgrowths. The subhedral ilmenite to the center-right is not in optical continuity with the host ilmenite. (b) ilmenite megacryst reaction rim with CMAT and perovskite. Lamellae of spinel in the megacryst core merge with the spinel in the rim. Sulfides are concentrated in the matrix surrounding the reaction rim. (c) Euhedral spinel in the groundmass. TMAC core is partially surrounded by ilmenite which, in turn, is mantled by CMAT with a thin rim of MAT and epitaxial overgrowths of perovskite. (d) Ilmenite megacryst reaction rim and groundmass spinel. Reaction rim contains unreacted remnants of ilmenite and euhedral overgrowths on spinels. The groundmass grains are zoned from TMAC–CMAT–MAT and are partially mantled by perovskite.

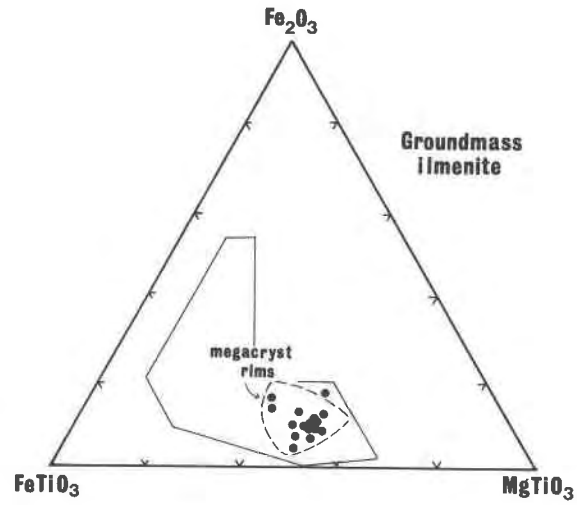

Fig. 4. Groundmass ilmenite compositions and range of ilmenite megacryst rim compositions (dashed line) plotted in the ilmenite ($FeTiO_3$)–geikielite ($MgTiO_3$)–hematite (Fe_2O_3) ternary. Solid line delineates the field of kimberlitic ilmenites defined by Mitchell (1977).

is partially mantled by ilmenite which, in turn, is mantled by brown spinel (Fig. 3c). Groundmass ilmenite may be partially or wholly mantled by perovskite. Rarely is it present without a rim of either perovskite or spinel, but when it is, the margin is fretted or resorbed.

Compositions of groundmass ilmenites and inclusions in olivine rims are plotted in the ilmenite ($FeTiO_3$)–hematite (Fe_2O_3)–geikielite ($MgTiO_3$) ternary (Fig. 4). Chemically, they are identical to the ilmenite megacryst rims. Mg-enriched rims are a common feature on kimberlitic ilmenite megacrysts (*e.g.*, Boctor and Meyer, 1979; Boctor and Boyd, 1980, Agee *et al.*, 1982; Haggerty *et al.*, 1979; Pasteris, 1980). Typically, groundmass ilmenites show chemical identity with the rim compositions, and it is generally accepted that they crystallized in equilibrium with the megacryst rims; however, the provenance of the ilmenite megacrysts themselves is a subject of debate.

Spinels

Spinels occur as discrete grains within the groundmass, as inclusions in silicates, in ilmenite megacryst reaction rims, and in garnet reaction rims. In the groundmass, they are euhedral to subhedral in form, although subskeletal and atoll habits are not uncommon. There is a seriate size distribution with the largest grains up to 100 μm. Zonation is present within the majority of the grains (Figs. 3c and d; compositions are shown in Fig. 5). Cores are of grey-blue titaniferous Mg-Al-chromite (TMAC) and zone continuously into tan-brown chromian Mg-Al-titanomagnetite (CMAT). Usually, a thin rim (2–5 μm wide) of higher-reflectance Mg-Al-titanomagnetite (MAT–strictly speaking, magnetite–ulvöspinel) is present. The TMAC cores may be absent in smaller grains. Chemically, the trend is not continuous; a compositional gap occurs towards the more Ti-rich end of the range (Fig. 5). With increasing TiO_2 contents, $Fe^{2+}/(Fe^{2+}+Mg)$ and MnO increase, and Fe^{3+} increases relative to Cr^{3+} and Al^{3+}; both Cr_2O_3 and Al_2O_3 decrease, but Al/(Al+Cr) increases.

Rare, euhedral inclusions of TMAC are present in Cr-rich olivine megacrysts. These inclusions are the most Cr-rich analyzed. The abundant spinel inclusions in phlogopite phenocrysts and phlogopite mantles on garnet reaction rims range from TMAC to CMAT in composition.

Spinel in ilmenite-megacryst reaction rims (Figs. 3a, b,

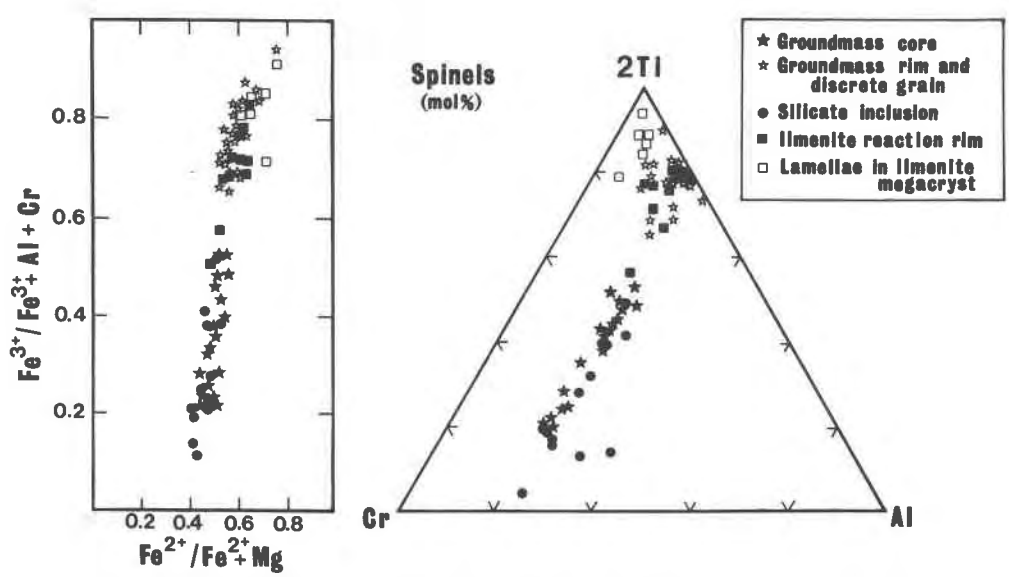

Fig. 5. Spinel compositions plotted in projections of the reduced (right) and normal (left) prisms.

and d) is of the CMAT–MAT variety, compositionally overlapping the more titanian groundmass compositions. Contacts between the spinel and host ilmenite are sharp but irregular. Adjacent to the matrix, spinels possess euhedral crystal forms (Figs. 3a and d) and a thin rim of MAT. Parallel lamellae of tan-brown spinel are present in the outer 200–300 μm of some of the ilmenite megacrysts (Fig. 3b). These lamellae extend into the reaction rims and merge, with no detectable boundary, into the spinel within the rim. Chemically, they are poorer in Cr_2O_3 and Al_2O_3 than the spinel in the reaction rims; this is to be expected, since the cores of the megacrysts from which these lamellae are exsolved are poorer in these components than the rims.

Secondary Ti-, Al-, and Cr-poor magnetite grains occur within serpentinized olivine megacrysts and in the matrix surrounding these pseudomorphs: those in the matrix possess rims of MAT.

In general, the spinel compositional trend is similar to those described from other kimberlites (*e.g.*, Haggerty, 1975; 1979; Elthon and Ridley, 1979; Mitchell and Clarke, 1976; Mitchell, 1979). In other kimberlites, spinel has been described that displays more restricted or different compositional trends (*e.g.*, Boctor and Meyer, 1979; Boctor and Boyd, 1980; Agee *et al.*, 1982). The spinels in the megacryst reaction rims are relatively evolved compared with groundmass core compositions. In reaction rims described by Elton and Ridley (1979) and Boctor and Meyer (1979), the spinels span the entire range of groundmass spinel compositions. In the Somerset Island kimberlites, Mitchell (1979) noted that spinels coexisting with phlogopites in the micaceous Tunraq kimberlite were relatively depleted in alumina compared to those in the Peuyuk and Elwyn Bay kimberlites. The spinel trend in the micaceous Fayette County kimberlite is more analogous to the micaceous Tunraq than the mica-poor kimberlites from Somerset Island, corroborating the observations of Mitchell. Although phlogopite does not control the Ti-enrichment in the fractionating melt (see above), it seems to have a major influence on the partitioning of alumina between spinel and melt.

Spinels in kelyphitic reaction rims on the garnet megacrysts are translucent brown Cr-pleonaste or green pleonaste. They are associated with aluminous, Ca-rich and Ca-poor pyroxenes (up to 14 wt.% Al_2O_3), olivine, and alkali-rich glass (up to 8 wt.% $Na_2O + K_2O$). They are either symplectically intergrown with pyroxene and glass or form skeletal-euhedral crystals within the glass. These reaction assemblages have formed as a result of incongruent melting of the garnets due to metasomatic addition of alkalis and volatiles. The textures, compositions, and interpretion of these assemblages are described in detail by Hunter and Taylor (1982).

Perovskite and rutile

Perovskite is present as finely-crystalline aggregates or as discrete grains. Within the groundmass, it occurs as partial or complete mantles on ilmenite or spinel, as discrete epitaxial grains on groundmass spinels (Figs. 3c and d), or as discrete euhedral grains, 10–20 μm in size. It is also a major component of the ilmenite megacryst reaction rims (Figs. 3a,b, and d), where it is present either as partial mantles on spinel or with an irregular contact adjacent to the host ilmenite. As with the spinels, perovskite adjacent to the matrix may possess euhedral crystal form.

Chemically, there is little difference between the groundmass perovskites and those in the ilmenite reaction rims. Only minor amounts of FeO* (<2%) were detected. This low Fe-content is characteristic of kimberlitic perovskites, indicating formation under conditions of low fO_2 (Mitchell, 1972; *cf.*, Kimura and Muan, 1971a;b). In general analysis totals were in the range 96–98%; REE's and Nb show minor peaks in energy dispersive spectra of these perovskites. These elements can be present in concentrations of several percent in kimberlitic and carbonatitic perovskites (*e.g.*, Mitchell, 1972; Boctor and Boyd, 1980; 1981; 1981).

Rutile occurs as fine, acicular needles (2 × 10 μm) throughout the matrix of this kimberlite.

Discussion

The intrinsic nature of oxides, especially ilmenite, being highly sensitive to changes in melt composition, fO_2, and temperature, permits their use in deciphering the conditions prevailing during the middle- to late-stages of kimberlite development.

Ilmenite instability

Reaction rims are a common feature on kimberlitic ilmenites (*e.g.*, Mitchell, 1972; Haggerty, 1973; Elthon and Ridley, 1979; Boctor and Meyer, 1979; Boctor and Boyd, 1980; Pasteris, 1980; Agee *et al.*, 1982). A variety of products may be present, but perovskite and spinel are most common. The abundance of perovskite in the reaction assemblage indicates a high aCa in the later stages of evolution of kimberlitic melts; this is a natural consequence of the absence of any major Ca-bearing liquidus phases throughout the mid-stages of fractionation. Reaction of the ilmenite with the Ca-rich melt releases Ti, which is taken up by perovskite, and Fe^{2+}, Fe^{3+}, Mg, Mn, Cr, and Al, which partition into the spinel phase. In addition, exotic elements may be taken up from the melt into the products, *e.g.*, REE and Nb into perovskite or rutile (Mitchell, 1972; Boctor and Meyer, 1979; Boctor and Boyd, 1980; 1982), or Ca-Cr-armalcolite (*e.g.*, Haggerty, 1975). A secondary ilmenite is sometimes present within the reaction products (*e.g.*, Haggerty, 1973; Agee *et al.*, 1982). No spinel was observed in reactions described by Mitchell (1972); it was suggested that silicates such as serpentine and chlorite accommodated excess Mg and Fe from the reaction.

Mineralogically, the reaction rims in the Fayette Coun-

ty kimberlite are relatively simple; only perovskite and spinel are present. Their compositions are similar to those phases in the groundmass. The occurrence of euhedral epitaxial overgrowths on perovskite and spinel adjacent to the matrix indicates that some portion of the assemblages are primary precipitates from the melt. Local buffering of fO_2 by reaction assemblages may lead to variations in Fe^{3+}/Fe^{2+} ratios within minerals in the same rim (Haggerty, 1973), and the reactions will lead to localized variations in Mg, Ti, and Al activities (Boctor and Meyer, 1979). Haggerty suggests that fO_2 will be controlled in late-stage melts by local variations in CO/CO_2 and H_2/H_2O. Local variations in fO_2 and fCO_2 could affect the aCa by dissolution or precipitation of carbonate, *i.e.*,

$$2CaCO_3 = 2Ca^{2+}_{fluid} + O_2 + CO_2$$

In the Fayette County kimberlite, variations in a Ca are suggested by the inhomogeneous distribution of primary perovskite within the groundmass and the wide ranges in modal percentages of perovskite in the reaction rims; the reaction products show a continuum from an assemblage composed entirely of ilmenite + pervoskite to one in which spinel is the only visible product. There is no evidence to suggest major variations in fO_2 in the late-stage melts but a low fO_2 is indicated by the low solubility of Fe in the perovskites (Mitchell, 1972); experiments in the system CaO–FeO–TiO_2 at varying oxygen fugacities (Kimura and Muan, 1971a,b) indicate that at higher fO_2 significant amounts of Fe are soluble in perovskites as Fe_2O_3.

The inhomogeneous distribution of sulfides within the matrix and the spatial association of sulfides in some of the reaction assemblages suggests that fS_2 was also variable on a local scale. These small scale differences in volatile-phase fugacities are to be expected during the volatile-rich later-stages of kimberlite evolution.

Crystallization sequence and melt chemistry

In order to place the petrology of the mid- and late-stage oxides and phlogopites within the context of the entire evolution of the Fayette County kimberlite, it is pertinent to briefly summarize the chemistry of the megacryst and inclusion suites reported by Hunter and Taylor (1984).

The *Cr-rich suite* is composed of olivine (Fo 93–90), Cr-garnet (1.6–6.2% Cr_2O_3; mg = 0.81–0.85), Cr-diopside (1.9–2.3% Cr_2O_3), enstatite (0.2–0.6% Cr_2O_3), titanian Mg–Al chromite (38–34% Cr_2O_3), and immiscible sulfide-melt products. The suite possesses a limited range of mg, and major element compositions are similar to those in sheared garnet lherzolite xenoliths. Minor element variations of the minerals are consistent with crystal fractionation from a Cr-rich kimberlitic melt over a temperature interval from 1310–1055°C in the pressure range 48–39 kbar. The *Cr-poor suite* is more evolved and comprises olivine (Fo 81–85), garnet (<0.1% Cr_2O_3; mg = 0.72), picroilmenite (16–37 mol% $MgTiO_3$; 0.05–2.05% Cr_2O_3) and diopside (<0.1% Cr_2O_3). Olivines of *both* populations have rim compositions of Fo 88–89, and ilmenite megacrysts possess reverse-zoned rims (34–51 mol% $MgTiO_3$; 1.4–3.6% Cr_2O_3). The Cr-rich and Cr-poor suites are analogous to those described from the Colorado–Wyoming kimberlites (Eggler *et al.*, 1979).

The presence of two intimately intermingled, chemically distinct megacryst/inclusion suites indicates that a mixing event must have occurred during the evolution of the kimberlite. Mineralogically, the mixing of the two populations and their host Cr-, Mg-rich and Cr-poor host melts, respectively, is manifest in the chemical zonation observed in the olivine and ilmenite megacryst rims (Hunter and Taylor, 1984). With the exception of the Cr-spinel inclusions in the Cr-rich olivine megacrysts, the oxides and phlogopites described herein are the products of crystallization of the hybrid kimberlitic melt.

The presence of ilmenite inclusions within the Cr-poor garnets led Hunter and Taylor (1984) to suggest that picroilmenite was part of the Cr-poor suite, a conclusion also reached by Eggler *et al.* (1979) in the Colorado–Wyoming kimberlites. The lack of significant Fe enrichment in the Cr-rich melt probably precluded ilmenite saturation within that melt. Clearly, the presence of ilmenite in the groundmass indicates that ilmenite was saturated in the hybrid melt subsequent to the mixing event. The compositional similarity of the groundmass ilmenite to the ilmenite megacryst rims suggests that growth of Mg-enriched ilmenite occurred on the ilmenite megacrysts, but the smooth compositional profile (Fig. 6 of Hunter and Taylor, 1984) of MgO towards the core-region indicates that diffusion was acting to re-equilibrate the cores.

The presence of TMAC mantled by ilmenite within the groundmass and its absence in the ilmenite reaction rims indicates that it was crystallizing prior to ilmenite saturation. The occurrence of euhedral TMAC as inclusions within Cr-rich olivine megacrysts suggests that it was a stable liquidus phase over a portion of the crystallization interval within the Cr-rich melt prior to its mixing with the ilmenite-saturated Cr-poor melt.

The specific timing of the appearance of phlogopite with respect to the mixing event is ambiguous. The abundance of euhedral TMAC inclusions in phlogopite phenocryst cores and in phlogopites mantling garnet reaction rims indicates that phlogopite became a liquidus phase subsequent to the appearance of TMAC. The presence of phlogopite mantles of similar composition on *both* Cr-garnets and Cr-poor garnets suggests that the appearance of phlogopite post-dates the mixing event. However, the highest Cr-contents observed in phlogopites are in the mantles on the Cr-garnets, suggesting perhaps that these Cr-phlogopites may slightly pre-date the mixing event.

Ilmenite, CMAT and phlogopite crystallized simulta-

neously during fractionation subsequent to the mixing event. Late-stage instability of ilmenite is indicated by the reaction to form perovskite. Perovskite, MAT and phlogopite are stable liquidus phases in the latest stages, with appearance of rutile just above the solidus.

The observed paragenetic sequence of oxides and phlogopites within the groundmass allows a qualitative reconstruction of the changes in chemical potential during the mid-, to late-stages of the evolution of this kimberlite. Both phlogopite and spinels record a decrease in Cr activity during fractionation. The spinels record an increase in Ti and Fe^{3+} activities, which are general features of kimberlitic groundmass spinels. The reaction of ilmenite to form perovskite and the appearance of perovskite as a stable liquidus phase indicates increased aCa and aTi and low aSi. The increase in aTi may be a consequence of the breakdown of ilmenite. The presence of rutile in the groundmass indicates high Ti activity in the latest melt. In addition to the increase in Ca (indicated by the precipitation of perovskite), phlogopites, apatite and zircon record increases in REE, Nb, P, Zr, and Na during fractionation.

Kimberlite evolution—a synopsis

The systematic chemical variations recorded by both the phlogopites and oxide phases of the Fayette County kimberlite are not typical of kimberlites in general. A number of points may be pertinent in this regard. First, this kimberlite would be termed a phlogopite–calcite kimberlite in the classification of Skinner and Clement (1979). Thus, the inferred systematics might only be applicable to kimberlites of this type (*i.e.*, in phlogopite-absent kimberlites, different trends in oxide phases might be expected). Second, this kimberlite is remarkably fresh; chemical variations have not been modified by deuteric alteration, as is common in diatreme-facies kimberlites. The freshness may be related to the hypabyssal nature of this kimberlite. Despite these differences, the synopsis for kimberlite evolution, as exemplified by the Fayette County occurrence, is probably applicable generally.

The two chemically distinct megacryst/inclusion populations record the differing evolutionary paths of the end-members involved in the mixing event. The Cr-poor megacrysts record the fractionation of a melt within magma chambers in the upper levels of the LVZ. This suite represents "normal" high-pressure fractional crystallization of a kimberlitic melt. Harte and Gurney (1981) have proposed a model in which fractionation occurs in magma sheets and apophyses surrounding a magma chamber. Their scenario allows the simultaneous existence of different stages of magma differentiation under essentially isobaric conditions. Conditions for effective melt segregation within the upper levels of the LVZ occur because of the presence of a thermal barrier on the solidus at depths of 120–80 km. Once optimum conditions to promote crack propagation occur (*i.e.*, volatile build-up and tension in the lithosphere), the solidus barrier may be breached. As a consequence, there will be little tendency for melts in newly rising diapirs to segregate. Under these conditions, where melt/crystal ratios are relatively low, fractionation paths of megacrysts are influenced by bulk-assimilation of mantle peridotite and/or by zone-refining processes. Major element compositions of melts in the diapirs will be buffered by the host mantle, and fractionating megacrysts will exhibit a limited range of *mg*. Additional factors affecting the crystallization paths of melts within the diapirs or within segregated melts will be ambient fO_2 and fS_2. In summary, the Cr-poor megacryst suite represents crystallization from segregated melts in the upper levels of the LVZ—the "nor-

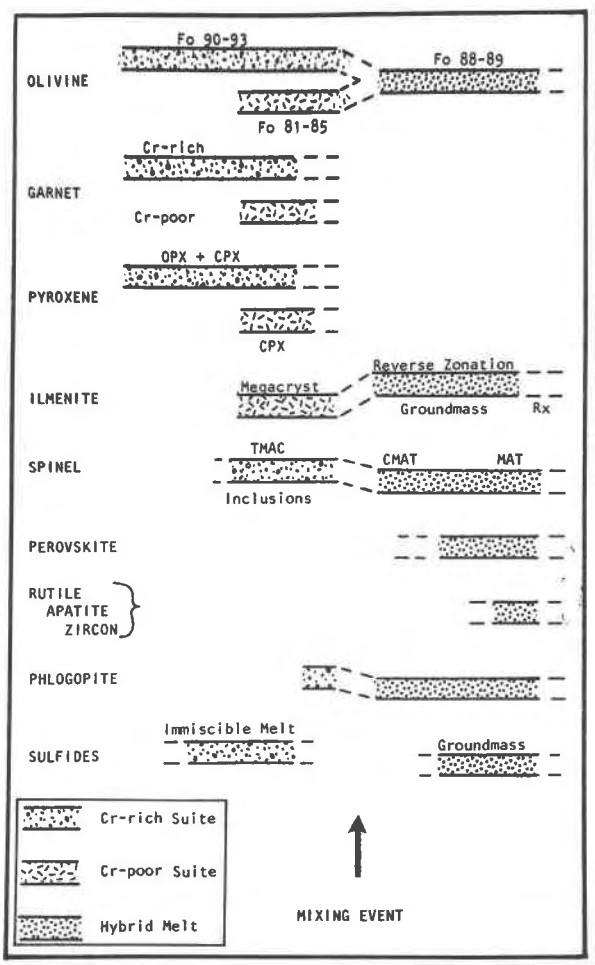

Fig. 6. Summary of the evolutionary stages of the Fayette County kimberlite. The left-hand side shows the phases present in the Cr-poor and Cr-rich suites. These populations represent the fractionation of the Cr-poor and Cr-rich melts in the LVZ (see Hunter and Taylor, 1984 and this text for details). The mixing event represents the disruption of the Cr-poor crystal mush by the uprising diapir bearing the Cr-rich melt/megacryst assemblage. The right-hand side shows the phases crystallizing from the hybrid kimberlite during its path through the upper mantle and crust (see text for details).

mal'' fractionation trend of increasing Fe^{2+} (Fe^{2+} + Mg), ultimately achieving ilmenite saturation. The Cr-rich suite represents an evolutionary path within a rising diapir where *mg* is buffered by the host mantle. The high Cr-contents may reflect partial melting of a heterogeneous source-region. The evolution of the two kimberlitic melts within the LVZ is summarized in the left-hand side of Figure 6.

During its movement upwards, the Cr-rich melt with its xenoliths and megacrysts disrupted the shallower, Cr-poor crystal mush. Thorough mixing of the host melts resulted in a hybrid melt. It was in this hybrid melt that the Mg-rich rims on the ilmenite megacrysts and the reverse and normal zonation on the olivine megacrysts formed. The fractionation of this hybrid melt is recorded by the chemical changes in the phlogopites and groundmass oxides and the stabilization of perovskite in place of ilmenite. This hybrid melt was the fluid kimberlitic medium that transported the mantle megacryst and xenolith assemblages through the upper mantle and crust. The evolution of the kimberlite during this stage is summarized in Figure 6.

Acknowledgments

Drs. N. Z. Boctor, J. D. Pasteris and J. V. Smith reviewed earlier versions of this paper. This research has also benefitted from the comments and suggestions of Drs. H. Y. McSween and O. C. Kopp. Financial assistance was provided by the University of Tennessee Department of Geological Sciences Discretionary Fund and NASA Grant NGL 43-001-140.

References

Agee, J. J., Garrison, J. R., Jr., and Taylor, L. A. (1982) Petrogenesis of oxide minerals in kimberlite, Elliott County, Kentucky. American Mineralogist, 67, 28–42.

Albee, A. L. and Ray, L. (1970) Correction factors for electron probe microanalysis of silicates, oxides, carbonates, phosphates and sulphides. Analytical Chemistry, 42, 1408–1414.

Bence, A. E. and Albee, A. L. (1968) Empirical correction factors for the electron microanalysis of silicates and oxides. Journal of Geology, 76, 382–403.

Boctor, N. Z. and Boyd, F. R. (1980) Oxide minerals in the Liahobong Kimberlite, Lesotho. American Mineralogist, 65, 631–638.

Boctor, N. Z. and Boyd, F. R. (1981) Oxide minerals in a layered kimberlite–carbonatite sill from Benfontein, South Africa. Contributions to Mineralogy and Petrology, 76, 253–259.

Boctor, N. Z. and Boyd, F. R. (1982) Petrology of kimberlite from the DeBryun and Martin Mine, Bellsbank, South Africa. American Mineralogist, 67, 917–925.

Boctor, N. Z. and Meyer, H. O. A. (1979) Oxide and sulphide minerals in kimberlite from Green Mountain, Colorado. In F. R. Boyd and H. O. A. Meyer, Eds., Kimberlites, Diatremes and Diamonds: Their geology, petrology and geochemistry, p. 217–228. American Geophysical Union, Washington, D.C.

Boettcher, A. L., O'Neil, J. R., Windom, K. E., Stewart, D. C. and Wilshire, H. G. (1979) Metasomatism of the upper mantle and the genesis of kimberlites and alkali basalts. In F. R. Boyd and H. O. A. Meyer, Eds., The Mantle Sample: Inclusions in kimberlites and other volcanics, p. 173–182. American Geophysical Union, Washington, D.C.

Clarke, D. B. and Mitchell, R. H. (1975) Mineralogy and petrology of the Somerset Island Kimberlite, N.W.T., Canada. Physics and Chemistry of the Earth, 9, 123–136.

Clement, C. R. (1973) Kimberlites from the Kao Pipe, Lesotho. In P. H. Nixon, Ed., Lesotho Kimberlites, p. 110–121. Lesotho National Development Corporation, Maseru.

Danchin, R. V., Ferguson, J., McIver, J. R., and Nixon, P. H. (1975) The composition of late-stage kimberlite liquids as revealed by nucleated autoliths. Physics and Chemistry of its Earth, 9, 235–245.

Dawson, J. B. (1980) Kimberlites and their Xenoliths. Springer Verlag, New York.

Delaney, J. S., Smith, J. V., Carswell, D. A., and Dawson, J. B. (1980) Chemistry of micas from kimberlites and xenoliths—II. Primary- and secondary-textured micas from peridotite xenoliths. Geochimica et Cosmochimica Acta, 44, 857–872.

Eggler, D. H., McCallum, M. E., and Smith, C. B. (1979) Megacryst assemblages in kimberlites from Northern Colorado and Southern Wyoming: Petrology, geothermometry, barometry, and areal distribution. In F. R. Boyd and H. O. A. Meyer, Eds., The Mantle Sample: Inclusions in Kimberlites and other volcanics, p. 213–126. American Geophysical Union, Washington, D.C.

Elthon, D. and Ridley, W. I. (1979) The oxide and silicate mineral chemistry of a kimberlite from the Premier Mine: Implications for the evolution of kimberlitic magmas. In F. R. Boyd and H. O. A. Meyer, Eds., Kimberlites, Diatremes, and Diamonds: Their geology, petrology, and geochemistry, p. 206–216. American Geophysical Union, Washington, D.C.

Emeleus, C. H. and Andrews, J. R. (1975) Mineralogy and petrology of kimberlite dike and sheet intrusions and included peridotite xenoliths from southwest Greenland. Physics and Chemistry of the Earth, 9, 179–198.

Ferguson, J., Danchin, R. V., and Nixon, P. H. (1973) Petrochemistry of kimberlite autoliths. In P. H. Nixon, Ed., Lesotho Kimberlites, p. 285–293. Lesotho National Development Corporation, Maseru.

Garrison, J. R., Jr., and Taylor, L. A. (1980) Megacrysts and xenoliths in Kimberlite, Elliott County, Kentucky: A mantle sample from beneath the Permian Appalachian Plateau. Contributions to Mineralogy and Petrology, 75, 27–42.

Gurney, J. J., Jakob, W. R. O., and Dawson, J. B. (1979) Megacrysts from the Monastery Kimberlite Pipe, South Africa. In F. R. Boyd and H. O. A. Meyer, Eds., The Mantle Sample: Inclusions in kimberlites and other volcanics, p. 227–243. American Geophysical Union, Washington, D.C.

Haggerty, S. E. (1973) Spinels of unique composition associated with ilmenite rechious in the Lighobong Kimberlite pipe, Lesotho. In P. H. Nixon, Ed., Lesotho Kimberlites, p. 149–158. Lesotho National Development Corporation, Maseru.

Haggerty, S. E. (1975) The chemistry and genesis of opaque minerals in kimberlite. Physics and Chemistry of the Earth, 9, 295–307.

Haggerty, S. E. (1979) Spinels in high-pressure regimes. In F. R. Boyd and H. O. A. Meyer, Eds., The Mantle Sample: Inclusions in kimberlites and other volcanics, p. 183–196. American Geophysical Union, Washington, D.C.

Haggerty, S. E., Hardie, R. B., McMahon, B. M. (1979) The mineral chemistry of ilmenite nodule associations from the Monastery diatreme. In F. R. Boyd and H. O. A. Meyer, Eds., The Mantle Sample: Inclusions in kimberlites and other vol-

canics, p. 249–256. American Geophysical Union, Washington, D.C.

Harte, B. and Gurney, J. J. (1981) The mode of formation of chromium-poor megacryst suites from kimberlites. Journal of Geology, 89, 749–753.

Hickock, W. O. and Moyer, F. T. (1940) Geology and mineral resources of Fayette County, Pennsylvania. Pennsylvania. Geological Survey Bulletin, v. 26, 4th Series, 153–159.

Hunter, R. H. and Taylor, L. A. (1984) Magma-mixing in the low velocity zone: Kimberlitic megacryst and inclusions from Fayette County, Pennsylvania. American Mineralogist, 69, 16–29.

Hunter, R. H. and Taylor, L. A. (1982) Instability of garnet from the mantle: Glass as evidence of metasomatism and melting. Geology, 10, 617–620.

Kimura, S. and Muan, A. (1971a) Phase relations in the system CaO–iron oxide–TiO_2 in air. American Mineralogist, 56, 1332–1346.

Kimura, S. and Muan, A. (1971b) Phase relations in the system CaO–iron oxide–TiO_2 under strongly reducing conditions. American Mineralogist, 56, 1347–1358.

Mitchell, R. H. (1972) Composition of perovskite in kimberlite. American Mineralogist, 57, 1748–1753.

Mitchell, R. H. (1977) Geochemistry of magnesian ilmenite from kimberlites in South Africa and Lesotho. Lithos, 10, 29–37.

Mitchell, R. H. (1979) Mineralogy of the Tunraq kimberlite, Somerset Island, N.W.T. Canada. In F. R. Boyd and H. O. A. Meyer, Eds., Kimberlites, Diatremes and Diamonds: Their geology, petrology, and geochemistry, p. 161–171. American Geophysical Union, Washington, D.C.

Mitchell, R. H. and Clarke, D. B. (1976) Oxide and sulphide mineralogy of the Penyuk Kimberlite, Somorset Island, N.W.T., Canada. Contributions to Mineralogy and Petrology, 56, 157–172.

Nixon, P. H. and Boyd, F. R. (1973). The discrete nodule (megacryst) association in kimberlites from northern Lesotho. In P. H. Nixon, Ed., Lesotho Kimberlites, p. 67–75. Lesotho National Development Corporation, Maseru.

Pasteris, J. D. (1980) The significance of groundmass ilmenite and megacryst ilmenite in kimberlites. Contributions to Mineralogy and Petrology, 75, 315–325.

Pasteris, J. D., Boyd, F. R., and Nixon, P. H. (1979) The ilmenite association of the Frank Smith Mine, R. S. A. In F. R. Boyd and H. O. A. Meyer, Eds., The Mantle Sample: Inclusions in kimberlites and other volcanics, p. 265–278. American Geophysical Union, Washington, D.C.

Pimental, N., Bikerman, M., and Flint, N. K. (1975) A new K–Ar date on the Masontown Dike, Southwestern Pennsylvanian. Pennsylvania. Geologist, 6, 5–7.

Rimsaite, J. (1971) Distribution of major and minor constituents between mica and host ultrabasic rocks and between zoned mica and zoned spinel. Contributions to Mineralogy and Petrology, 33, 259–272.

Roen, J. B. (1968) A transcurrent structure in Fayette and Green counties, Pennsylvania. United States Geological Survey Professional Paper, 600-C, 149–152.

Skinner, E. M. W. and Clement, C. R. (1979) Mineralogical clarification of South African kimberlites. In F. R. Boyd and H. O. A. Meyer, Eds., Kimberlites, Diatremes, and Diamonds: Their geology, petrology and geochemistry, p. 129–139. American Geophysical Union, Washington, D.C.

Smith, L. B. (1912) A peridotite dike in Fayette and Green Counties. Topographical and Geological Survey of Pennsylvania 1910–1912, Appendix F, 150–156.

Smith, J. V., Brennesholtz, R., and Dawson, J. B. (1978) Chemistry of micas from kimberlites and xenoliths. I. Micaceous kimberlites. Geochimica et Cosmochimica Acta, 42, 957–971.

Smith, J. V., Hervig, R. L., Ackermand, D., and Dawson, J. B. (1979) K. Rb, and Ba in micas from kimberlite and peridotite xenoliths and implications for the origin of basaltic rocks. In F. R. Boyd and H. O. A. Meyer, Eds., Kimberlites, Diatremes and Diamonds: Their geology, petrology, and geochemistry, p. 241–251. American Geophysical Union, Washington, D.C.

Sosman, R. B. (1938) Evidence on the intrusion-temperature of peridotites. American Journal of Science, 35, 353–359.

Manuscript received, July 19, 1982;
accepted for publication, May 24, 1983.